Transition-Metal Complexes with the Novel Poly(1,2,4-triazolyl)borate Ligands $[H_nB(C_2H_2N_3)_{4-n}]^-$ (n = 1 and 2): Synthesis and Characterization of Metal Complexes of Dihydrobis(1,2,4-triazolyl)borate as One- or Two-Dimensional Coordination Polymers with Six-Membered Ring Water Substructures and the Structure of Two-Dimensional Liquid and Solid Water As Organized in the Intercalate $[Ni\{HB(C_2H_2N_3)_3\}_2] \cdot 6\ H_2O$ (X-ray Studies at 293 and 160 K)☆

Christoph Janiak*[a], Tobias G. Scharmann[a], Holger Hemling[a], Dieter Lentz[b], and Joachim Pickardt[a]

Institut für Anorganische und Analytische Chemie, Technische Universität Berlin[a], Straße des 17. Juni 135, 10623 Berlin, Germany

Institut für Anorganische und Analytische Chemie, Freie Universität Berlin[b], Fabeckstraße 34–36, 14195 Berlin, Germany

Received September 20, 1994

Key Words: Poly(triazolyl)borates, metal complexes of / Coordination polymers / Water, cluster model / Water, two-dimensional structure / Hydrogen bonding

The 1:2 manganese (**5**), nickel (**6**), and copper complex (**7**) with the novel dihydrobis(1,2,4-triazolyl)borate ligand (**2**) were synthesized and structurally characterized. Single-crystal X-ray studies reveal the formation of highly solvated coordination polymers of the formula $\{[M(H_2O)_2\{\mu\text{-}H_2B(C_2H_2N_3)_2\}_2] \cdot n\ H_2O\}_\infty$ for M = Mn and Cu. In **5** (M = Mn; n = 4) a two-dimensional metal-ligand framework is built by means of the bridging action of **2**. These metal-ligand grid sheets sandwich water layers which comprise individual six-membered rings. Compound **7** (M = Cu; n = 6) can be described as a linear metal-ligand chain with two borate ligands bridging two copper centers. These one-dimensional coordination polymers are separated by one-dimensional arrays of water molecules in the form of edge-sharing six-membered rings. In both structures the water of crystallization is held in place both by hydrogen bonding from the aqua ligands and by hydrogen bonding to the nitrogen atoms of the borate ligand. Bis[hydrotris(1,2,4-triazolyl)borato]nickel, $[Ni\{HB(C_2H_2N_3)_3\}_2]$ (**8**), was obtained from $NiCl_2$ and the potassium salt of $[HB(C_2H_2N_3)_3]^-$ (**1**). Single-crystal X-ray structures of the solvate **8** · 6 H_2O were determined at 293 and 160 K. The water molecules are arranged in two-dimensional layers with only weak (hydrogen bonding) interactions to the adjacent layers of the complex molecules. The room temperature structure (orthorhombic, space group *Cmca*) shows a highly disordered water structure being indicative of a dynamic equilibrium between small conglomerates and free molecules. Upon cooling an ordering occurs in the water layer leading to a phase transition in the crystal, and in the low-temperature structure at 160 K (orthorhombic, space group *Pmnb*) the hydrogen atoms and bonding network of the water structure could be determined. This structure is best described as being composed of individual rings or chain segments. The material surface morphology after loss of the water of crystallization was studied by scanning electron microscopy and the structural pattern correlated with the crystal packing.

We have engaged in studies of the coordination chemistry of the potentially ambidentate poly(triazolyl)- and -(tetrazolyl)borate anions $[HB(C_2H_2N_3)_3]^-$ (**1**)[1–4], $[H_2B(C_2H_2N_3)_2]^-$ (**2**), and $[H_2B(CHN_4)_2]^-$ (**3**)[1,5,6]. These systems can be viewed as modifications of the thoroughly investigated chelating poly(*pyrazolyl*)borate ligands $[HB(pz)_3]^-$ and $[H_2B(pz)_2]^-$ (pz = pyrazolyl)[7]. The ligand **1** has been found to function mainly as a tris-chelate by coordination through the endodentate nitrogen donors[1–3,8], whereas in the transition-metal complexes of **3** the formation of 2-D coordination polymers has been the sole structural motif observed so far[5,6]. While the tridentate chelating action of **1** is analogous to $[HB(pz)_3]^-$ and may seem straight-foward, an AM1 theoretical calculation actually assigns a higher electrostatic potential and negative charge (−0.19 versus −0.11) to the exodentate N nucleophiles[1,3]. Although these exodentate donors play a part in the crystal packing by hydrogen bonding to solvent molecules of crystallization, they have only been observed once in a metal coordination: A case of linkage isomerism in the zinc complex[3] has revealed the formation of the molecular chelate complex and a three-dimensional coordination polymer, the latter being built up by the borate **1** bridging three zinc centers by the exodentate nitrogen atoms. The reaction conditions for the crystallization of the coordination polymer suggest this allotrope to be the thermodynamically more stable modification in accordance with the theoretical calculation and posed the question if the normally observed ready formation of chelate complexes of **1** should be explained by a combination of chelate and ki-

  0009–2940/95/0303–0235 $ 10.00+.25/0

netic effects[3]. For a better understanding of the effects influencing the coordination mode of **1** we have, thus, synthesized the dihydrobis(1,2,4-triazolyl)borate ligand **2** and transition-metal complexes thereof.

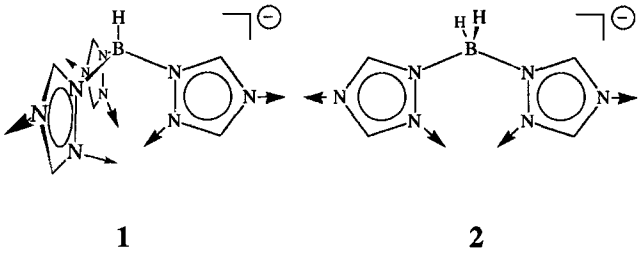

1 **2**

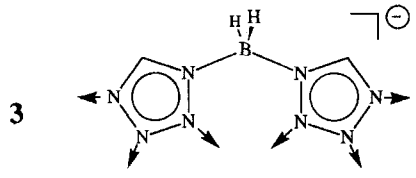

3

Furthermore, the crystal phases of transition-metal complexes with the novel multidentate poly(azolyl)borate ligands **1**[1-3], **3**[6], and as we will see here **2**, are often stabilized by solvent molecules. Those nitrogen donor atoms in **1**–**3** which are not utilized for metal coordination can interact with the solvent molecules such as water or methanol by hydrogen bonding and carry over some of the solvent-solute interaction to the solid state upon crystallization. In the tris(triazolyl)borate complexes $[M\{HB(C_2H_2N_3)_3\}_2] \cdot 6\ H_2O$ with M = Fe, Co, Zn[1,3] and $[Cu\{HB(C_2H_2N_3)_3\}_2] \cdot 4\ CH_3OH$[2] and in the bis(tetrazolyl)borate compounds $\{[M(H_2O)_2\{\mu\text{-}H_2B(CHN_4)_2\}_2] \cdot 2\ H_2O\}_\infty$ (M = Mn, Fe, Co, Zn, and Cd) two of the solvent molecules in each case are hydrogen-bonded to nitrogen atoms[6].

The fundamental importance of water drives a quest for a detailed understanding of the intermolecular forces and dynamics of the hydrogen bonding networks that operate in the condensed phases of water[9]. Hydration together with hydrogen bonding is not just crucial and has been intensively investigated in biological processes[10] but is important in inorganic systems as well[11].

In the case of $[M\{HB(C_2H_2N_3)_3\}_2] \cdot 6\ H_2O$ the water substructure presents itself as a two-dimensional layer with very weak interactions to the adjacent layers of complex molecules. For a better understanding of this 2-D water structural feature and its hydrogen bonding network we have performed a comparative structural study of the nickel complex $[Ni\{HB(C_2H_2N_3)_3\}_2] \cdot 6\ H_2O$ (**8** · $6\ H_2O$) at two different temperatures.

Syntheses and Properties of $K[H_2B(C_2H_2N_3)_2]$ (4) and $\{[M(H_2O)_2\{\mu\text{-}H_2B(C_2H_2N_3)_2\}_2] \cdot n\ H_2O\}_\infty$ with M = Mn (5, n = 4), Ni (6), and Cu (7, n = 6)

According to the general synthesis of poly(azolyl)borates[7,12], potassium boranate (KBH_4) reacts with 1,2,4-triazole in a 1:2 mixture at about 125°C with evolution of two mol of H_2 and formation of **4** as a white solid [Eq. (1)].

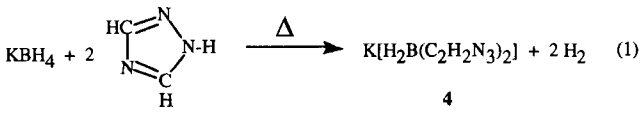

$$KBH_4 + 2 \xrightarrow{\Delta} K[H_2B(C_2H_2N_3)_2] + 2\,H_2 \quad (1)$$

4

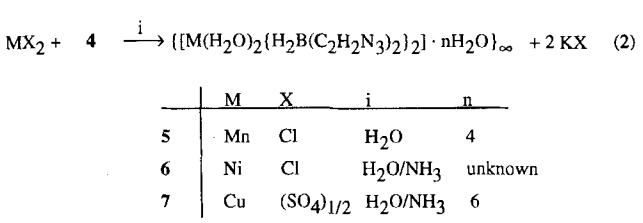

$$MX_2 + 4 \xrightarrow{i} \{[M(H_2O)_2\{H_2B(C_2H_2N_3)_2\}_2] \cdot nH_2O\}_\infty + 2\,KX \quad (2)$$

	M	X	i	n
5	Mn	Cl	H_2O	4
6	Ni	Cl	H_2O/NH_3	unknown
7	Cu	$(SO_4)_{1/2}$	H_2O/NH_3	6

The dihydrobis(triazolyl)borate anion (**2**) in the form of its potassium salt (**4**) reacts with manganese(II) and nickel(II) chloride or copper(II) sulfate in water with the formation of diaquabis[μ-dihydrobis(triazolyl)borato]metal(II) complexes [Eq. (2)]. Upon slow diffusion of solutions of the reactants the manganese compound **5**, together with water of crystallization, is obtained as colorless crystals directly from the reaction mixture in low yield while the nickel and copper compound precipitate initially only as an amorphous blue-violet or dark blue powder under the same conditions. The nickel and copper compound are, however, soluble in aqueous ammonia (presumably with formation of ammine-metal complexes) from which they crystallize upon slow solvent evaporation as violet needles (**6**) or blue platelets (**7**). We believe that there is an equilibrium between the ammine and the azolyl complex which is shifted during concentration and evaporation of ammonia to the latter.

X-ray structural investigations show that the crystals of **5** contain four, those of **7** six molecules of hydrogen-bonded water of crystallization per formula unit. The crystals of **5**–**7** more or less quickly eliminate the incorporated solvent of crystallization when taken out of the aqueous phase. Except for the solubility of **6** and **7** in aqueous ammonia, the bis(triazolyl)borato transition-metal complexes are insoluble in water or organic solvents once they have formed. Aside from the loss of water of crystallization the compounds are thermally stable to over 200°C. The infrared spectra reflect the ligand moiety. The quality of the nickel crystals **6** did not allow the collection of a crystallographic data set, however, from a comparison with the IR spectra of **5** and **7** we suggest a structure similar to the manganese compound **5**.

Temperature-variable magnetic measurements of **5** and **7** show a Curie-Weiss behavior of normal paramagnets in the temperature range measured (14–310 K). There is no magnetic coupling transmitted through the ligand, nor is there a through-space interaction of the metal centers (shortest M-M contacts are 8.14 and 8.92 Å for **5** and 8.84 or 9.27 for **7**). The magnetic moments are temperature-independent within experimental error and lie within the range typically observed for d^5 (high-spin, μ = 5.7–6.0 μ_B) or d^9 complexes (μ = 1.8–2.1 μ_B)[13].

Synthesis and Properties of $[Ni\{HB(C_2H_2N_3)_3\}_2] \cdot 6\ H_2O$ ($8 \cdot 6\ H_2O$) and $[Ni\{HB(C_2H_2N_3)_3\}_2]$ (8)

The hydrotris(1,2,4-triazolyl)borate anion **1** in the form of its potassium salt reacts with nickel(II) chloride in water with the formation of bis[hydrotris(triazolyl)borato]nickel(II) **8** [Eq. (3)]. Upon slow diffusion of solutions of the reactants the complex together with solvent of crystallization is obtained as red-violet crystals directly from the reaction mixture in 60% yield.

$$NiCl_2 + 2\ K[HB(C_2H_2N_3)_3] \rightarrow \underset{\mathbf{8}}{[Ni\{HB(C_2H_2N_3)_3\}_2]} + 2\ KCl \quad (3)$$

An X-ray structural investigation shows that the crystals of **8** contain six molecules of water per formula unit. Since the incorporated solvent is quickly eliminated when the crystals are taken out of the aqueous phase, the resulting surface morphology was studied by scanning electron microscopy (see below). Complex **8** is only very sparingly soluble in polar solvents such as water, methanol, dichloromethane, or chloroform and insoluble in nonpolar organic solvents like toluene or hexane.

Compound **8** is thermally stable to above 260°C (melting or decomposition point undetermined). In the mass spectrum the molecular ion is the base peak. The most likely fragmentation is loss of two triazolyl moieties and a hydrogen atom to give the second most abundant peak. Another prominent peak is due to loss of the hydrotris(triazolyl)borate radical leading to the mono(ligand)metal cation. Fragmentations of the molecular ion, $ML_2^{+\bullet}$, and ML^+ are very similar to other tris(triazolyl)metal complexes[2] involving loss of one or two triazolyl rings together with H, 2H, and/or HCN.

A temperature-variable magnetic measurement of **8** shows the expected Curie-Weiss behavior over the temperature range measured. The magnetic moment (μ = 3.0 μ_B at 300 K) is temperature-independent within experimental error and lies within the range typically observed for nickel complexes (μ = 2.9–3.9 μ_B, calculated spin-only value μ = 2.83 μ_B)[13].

X-Ray Structure of 5 and 7

Compounds **5** and **7** represent themselves as two- or one-dimensional coordination polymers, respectively. The arrangement of the metal centers and ligands within the layer structure of **5** is illustrated in Figure 1, for the linear, "columnane"-type chain[15] of **7** in Figure 2. The metal coordination in **5** together with the atom numbering scheme is detailed in Figure 3. The metal centers in both the manganese and copper complex are octahedrally coordinated, with the coordination polyhedron being formed from four nitrogen atoms of the bis(triazolyl)borate ligands and two *trans*-coordinated aqua ligands. The Jahn-Teller distortion in the d^9-Cu complex **7** manifests itself in an elongation of the Cu–OH_2 bonds (cf. Table 1). Only the exodentate nitrogen atoms of **2** function as donor atoms to the metal centers in **5** and **7**, in agreement with the charge distribution resulting from an AM1 calculation on the poly(triazolyl)borate ligands[1,3]. Thus, in contrast to the bidentate dihydrobis(*pyrazolyl*)borate ligand but similar to the dihydrobis(*tetrazolyl*)borate ligand **3**, the dihydrobis(*triazolyl*)borate system **2** does not form chelates but generates bridges between metal atoms. Selected bond lengths and angles for **5** and **7** are collected in Table 1. The B–N, C–N, and N–N bond length and angle variations are as seen before in the metal structures of **1**[2,3].

Figure 1. View from above a metal-complex layer of **5** (PLUTON-plot[4]). The solvate water has been omitted for clarity

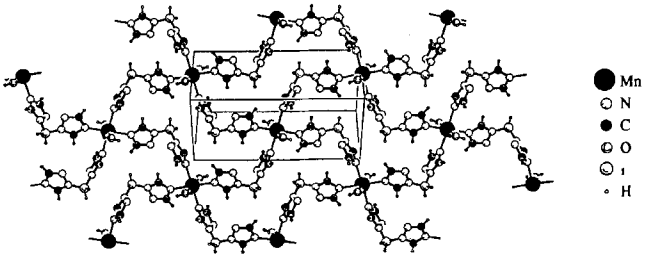

Figure 2. Metal-ligand chain in **7** with the atomic numbering scheme (50% probability ellipsoids, PLATON-TME plot[14])

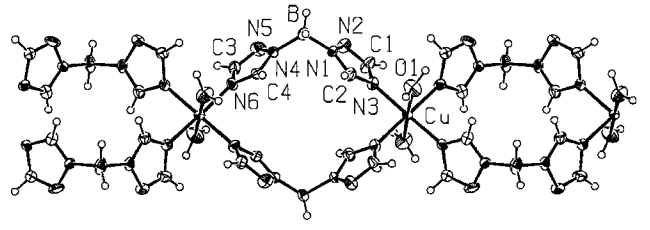

Figure 3. Metal coordination and atomic numbering scheme in the manganese complex **5** (PLATON-TME plot[14])

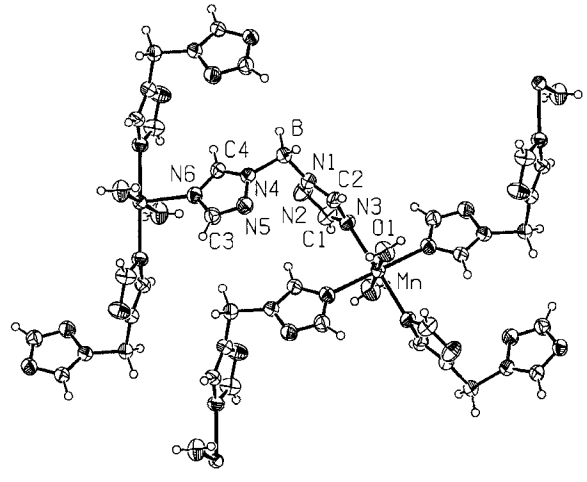

The coordination mode of **2** towards the metal centers supports the AM1-based relative order of the charge densities for the nitrogen donor atoms. To return to the starting point of our investigations: It appears to be the *tris*-chelating action in **1** that can successfully compete with the more thermodynamically favored exodentate coordination, while the *bis*-dentate chelate effect in **2** is no longer strong enough to overcome the charge-dictated ligating requirements.

A further important aspect in the discussion of the crystal structures of **5** and **7** is the stabilization of the crystal

Table 1. Selected bond distances [Å] and angles [°] for **5** and **7**

5 [a]		**7** [b]	
Mn-O1	2.183(3)	Cu-O1	2.396(7)
Mn-N6b	2.234(2)	Cu-N6b	2.016(6)
Mn-N3	2.265(3)	Cu-N3	2.014(7)
N6-Mn.d	2.234(2)	N6-Cu.d	2.016(6)
B-N1	1.562(5)	B-N1	1.585(14)
B-N4	1.574(4)	B-N4	1.55(2)
N1-C2	1.318(4)	N1-C2	1.318(12)
N1-N2	1.377(4)	N1-N2	1.369(11)
N2-C1	1.331(4)	N2-C1	1.281(13)
C1-N3	1.347(5)	C1-N3	1.340(13)
N3-C2	1.336(4)	N3-C2	1.300(12)
N4-C4	1.323(4)	N4-C4	1.310(12)
N4-N5	1.377(4)	N4-N5	1.372(11)
N5-C3	1.323(4)	N5-C3	1.291(12)
C3-N6	1.343(4)	C3-N6	1.351(12)
N6-C4	1.334(4)	N6-C4	1.317(12)
O-Mn-N	88.1(1)-91.9(1)	O-Cu-N	86.8(4)-94.2(4)
trans O-Mn-O	180	*trans* O-Cu-O	178.5(4)
trans N-Mn-N	180	*trans* N-Cu-N	177.1(4)
cis N-Mn-N	87.9(1), 92.1(1)	*cis* N-Cu-N	89.9(4)-90.1(2)
N1-B-N4	105.8(3)	N1-B-N4	108.6(8)

[a] Symmetry transformations used to generate equivalent atoms: $b = -x + 1/2, y + 1/2, -z + 3/2$; $d = -x + 1/2, y - 1/2, -z + 3/2$. – [b] Symmetry transformations used to generate equivalent atoms: $b = x, -y + 3/2, z + 1/2$; $d = -x + 1/2, y, z - 1/2$.

phase by solvent molecules as has been observed already in metal structures of the other novel poly(azolyl)borates **1** and **3**[1-3,6]. The nitrogen donor atoms in **1**–**3** which are not utilized for metal coordination can interact with the solvate molecules such as water (or in one case methanol) by hydrogen bonding and carry over some of the solvent-solute interaction to the solid state upon crystallization. In **2**, water molecules are hydrogen-bonded to both endodentate nitrogen atoms. As a consequence the metal complex layers in **5** are separated by layers of water molecules (alternatively, the metal complex grid sheets sandwich the water layer) and so are the metal-ligand columns in **7**. A stereoview and a packing diagram of the crystal structures in Figures 4 and 5, respectively, illustrate the layer- and channel-type inclusion phenomena[16] in **5** and **7**, respectively, which can also be described as clathrates[17].

The quality of the room-temperature data set of **5** allowed the determination of the hydrogen bonding network around the water molecules. Their hydrogen atoms were located and their positions refined. The potential hydrogen bond lengths and angles of the short intermolecular contacts are given in Table 2. Figure 6 presents a view of the water layer from above, including the hydrogen-bonded nitrogen atoms of the triazolyl rings (shaded circles). The water layer in **5** is built up by separate rings comprised of six oxygen atoms in a chair conformation with heterodromic[18] hydrogen-bonded circles. Each of the water species is threefold coordinated (when including the nitrogen and metal acceptors), and the water of crystallization donates one H bond to the "surface", i.e. to a nitrogen atom, of either one of the neighboring metal-ligand layers.

In the water substructure of **7** most, but not all, hydrogen atoms could be located with certainty. Therefore, only the O···O contacts of the potential hydrogen bonds are shown in Figure 7. A list of these short contacts is included in Table 2. The water structure in **7** is built up from rings of six oxygen atoms sharing opposite edges, reminiscent of a band or ladder polymer such as polyacene. Water aggregates as rings comprised of five or six O atoms are formed preferentially for topological reasons. The O···O distances shown in the water substructures of Figures 6 and 7 lie within the normal range of 2.6 to 3.0 Å[18]. The H···O/N contacts in Figure 6 between 1.81 and 2.13 Å are considerably shorter than the sum of the van der Waals radii of 2.6 for H and O or 2.7 for H and N[19].

Figure 5. Packing diagram of the crystal structure of **7** illustrating the tubulation of water columns inbetween and parallel to the metal ligand chains (PLUTON[14])

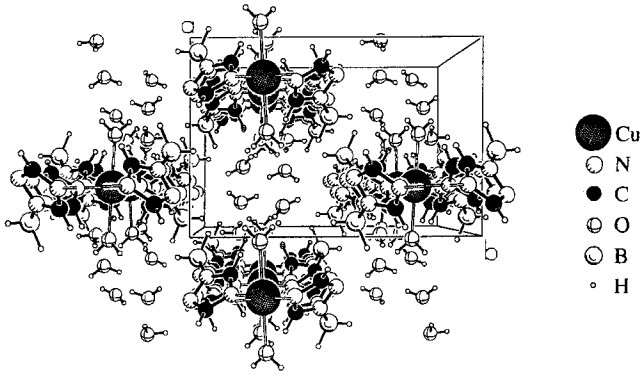

Figure 4. Stereoview of the crystal structure of **5** illustrating the intercalation of a water layer between the metal ligand grid sheets (PLUTON[14])

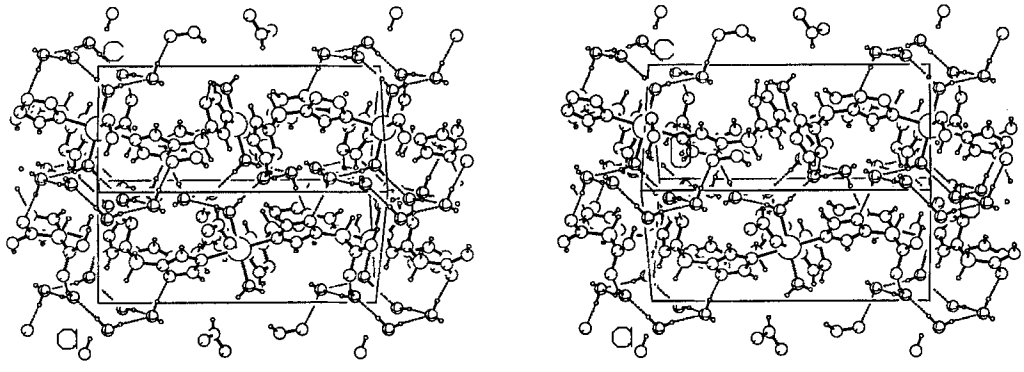

Table 2. Hydrogen-bonding schemes in compounds **5** and 7

5 [a] Donor–H···Acceptor	D···A [Å]	D–H [Å]	H···A [Å]	D–H···A [°]
O1-H10···O2	2.694(4)	0.88(5)	1.81(5)	173(5)
O1-H11···O3	2.847(4)	0.81(3)	2.05(4)	167(4)
O2-H20···N2e	3.031(5)	0.92(5)	2.13(5)	165(4)
O2-H21···O3f	2.858(5)	0.92(5)	1.96(5)	166(5)
O3-H31···N5f	2.796(5)	0.96(5)	1.85(5)	173(5)

7 [b] Donor(–H) ···Acceptor	D···A [Å]	Donor(–H) ···Acceptor	D···A [Å]
O1···O2	2.81(1)	O3···O3g	2.79(1)
O1···O3	2.81(1)	O4···O2	2.78(1)
O2···O4	2.78(1)	O2···O2g	2.73(1)
O2···N5e	2.90(1)	O3···O4h	2.75(1)
O3···N2f	2.93(1)	O4···O3b	2.75(1)

[a] Symmetry transformations used to generate equivalent atoms: $e = x, y, z - 1$; $f = -x + 1, -y + 1, -z + 1$. – All other O···O contacts are above 3.56 Å, the O···N contacts above 3.29 Å. – [b] Symmetry transformations used to generate equivalent atoms: $b = x, -y + 3/2, z + 1/2$; $e = x + 1/2, -y + 1, -z + 1/2$; $f = -x + 1, y + 1/2, -z + 1/2$; $g = -x + 3/2, -y + 3/2, z$; $h = x; -y + 3/2, z - 1/2$. – All other O···O contacts are above 3.86 Å, the O···N contacts above 3.31 Å.

Figure 6. View from above of a water layer in compound **5** with the hydrogen bonding network (dashed lines) and including the hydrogen-bonded nitrogen atoms of the triazolyl rings (shaded circles, PLUTON[14]). The atomic numbering scheme is illustrated; for symmetry labels see Table 2

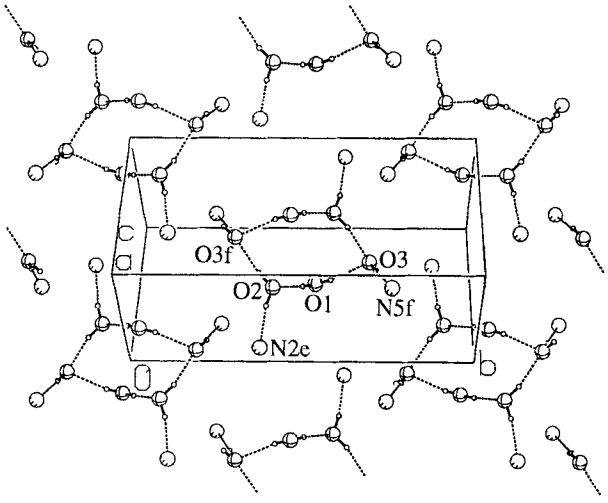

X-Ray Structure of 8 · 6 H_2O

The molecular structure of **8** is shown in Figure 8. The borate ligand functions as a tridentate chelate through the endodentate nitrogen donors to give octahedrally coordinated nickel. Selected bond distances and angles are compiled in Table 3. There is no change in the nickel coordination polyhedron when going to lower temperature, aside from a lower crystal symmetry (*Pmnb* versus *Cmca*) which removes the inversion symmetry from the nickel center and generates two independent borate ligands. The nickel octahedra are arranged in layers separated by layers of water molecules. The facile loss of the water when the crystal is removed from solution indicates, however, rather weak solvent-solute interactions. A stereoview of the crystal structure (Figure 9) illustrates the formation of this intercalate- or layer-type clathrate[17].

Figure 7. View of a water chain (oxygen centers only, crossed circles) in compound 7 with the short intermolecular contacts as dashed lines and including the hydrogen-bonded nitrogen atoms of the triazolyl rings as well as the coordinated copper atoms (PLUTON[14]). The atomic numbering scheme is illustrated; for symmetry labels see Table 2

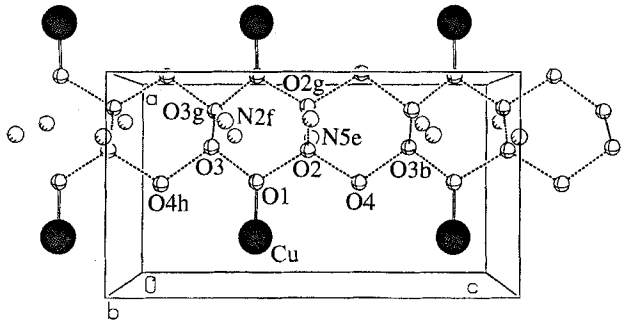

Figure 8. Molecular structure of $[Ni\{HB(C_2H_2N_3)_3\}_2]$ in **8** · 6 H_2O. The atomic numbering refers to the room-temperature structure (50% probability ellipsoids, PLATON-TME plot[14]); in the isostructural low-temperature form the borate ligands are no longer symmetry-related

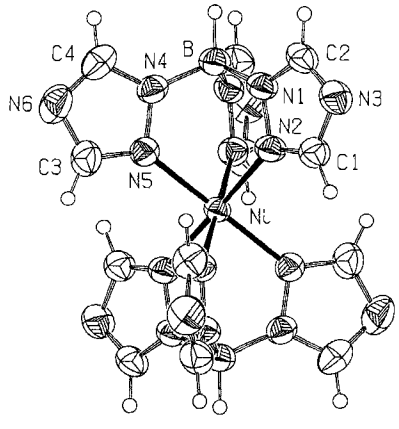

The change in temperature leads to an ordering in the water layer to which we ascribe the phase transition leading to the difference in space groups. The packing of the oxygen centers within the layer at the two temperatures is illustrated in Figure 10. At 293 K all water molecules except for the N···H–O–H···N-fixed ones (dark circles) are disordered. This disorder is a manifestation of the high thermal mobility and the dynamic behavior of liquid water. If an O···O distance in the range of about 2.6 to 3.0 Å is assumed for hydrogen bonding[18], the time-averaged structure of the two-dimensional aqueous phase has to be described by small H_2O clusters and isolated H_2O molecules. Such a description would be consistent with the Nemethy-Scheraga model discussed for liquid water[20].

A significantly reduced disorder is apparent for the low-temperature structure (Figure 10 and 11). The quality of

Figure 9. Stereoview of the crystal structure of **8** · 6 H_2O (low temperature) illustrating the intercalation of a two-dimensional water layer between metal complex layers (PLUTON plot[14])

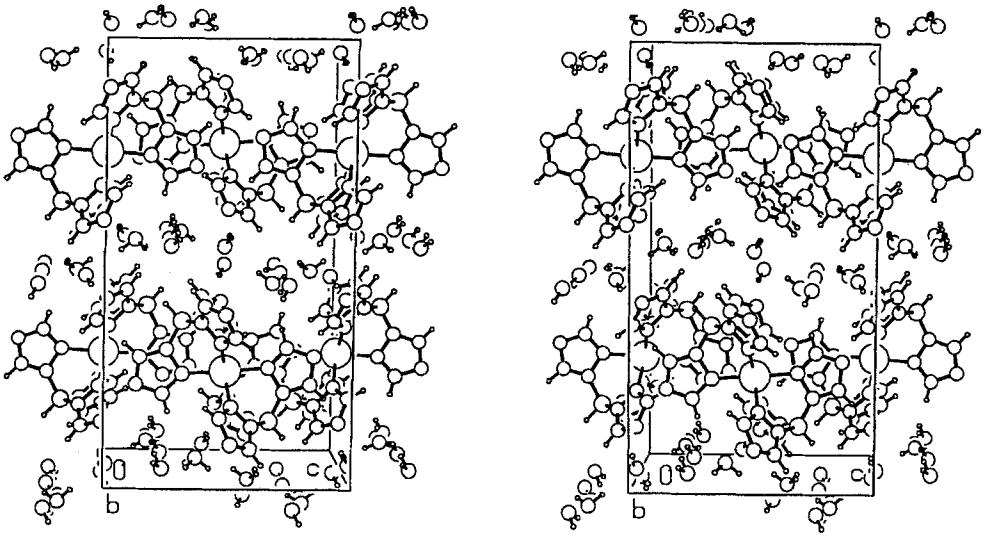

Table 3. Selected bond distances [Å] and angles [°] for complex **8** at 293 and 160 K

T = 293 K [a]		T = 160 K [b]			
Ni—N2	2.087(3)	Ni—N2	2.071(5)	Ni—N8	2.080(5)
Ni—N5	2.094(2)	Ni—N5	2.088(3)	Ni—N11	2.089(3)
B—N1	1.544(5)	B1—N1	1.527(8)	B2—N7	1.560(9)
B—N4	1.542(3)	B1—N4	1.547(5)	B2—N10	1.531(6)
N1—C2	1.331(4)	N1—C2	1.343(7)	N7—C6	1.306(8)
N1—N2	1.376(3)	N1—N2	1.376(6)	N7—N8	1.377(7)
N2—C1	1.315(4)	N2—C1	1.303(7)	N8—C5	1.309(8)
C1—N3	1.349(4)	C1—N3	1.365(8)	C5—N9	1.338(8)
N3—C2	1.325(5)	N3—C2	1.331(8)	N9—C6	1.309(9)
N4—C4	1.335(3)	N4—C4	1.334(5)	N10—C8	1.328(7)
N4—N5	1.370(3)	N4—N5	1.371(4)	N10—N11	1.369(5)
N5—C3	1.318(3)	N5—C3	1.312(5)	N11—C7	1.311(6)
C3—N6	1.349(4)	C3—N6	1.349(5)	C7—N12	1.346(6)
N6—C4	1.329(4)	N6—C4	1.323(5)	N12—C8	1.309(8)
trans N—Ni—N	180.0	*trans* N—Ni—N	179.4(2)		
cis N—Ni—N	86.04(9)-93.96(9)	*cis* N—Ni—N	86.2(1)-94.1(1)		
N1—B—N4	107.6(2)	N1—B1—N4	108.2(3)	N7—B2—N10	107.7(4)
N4—B—N4c	106.8(3)	N4—B1—N4a	108.8(2)	N10—B2—N10a	108.3(5)

[a] Symmetry operations: $c = -x + 1, y, z$. — [b] Symmetry operations: $a = x, -y + 1/2, z$.

this low-temperature data set allowed the determination of the hydrogen bonding network around the water molecules. The hydrogen atoms of the latter were located and their positions refined. The potential hydrogen bond lengths and angles of the short intermolecular contacts are given in Table 4. Figure 11 presents an on-top view of the water layer including the hydrogen-bonded nitrogen atoms of the triazolyl rings (shaded circles). Note the positional disorder of one hydrogen on O2 and the two-site position of O5. At both temperatures it is evident that two out of the six H_2O molecules per formula unit form hydrogen bonds to four exodentate nitrogen atoms. Even at low temperature, however, the water layer in **8** · 6 H_2O is not built up from edge-sharing O_6 rings (as in ice structures[21]) which have been observed in structures with stronger host-guest interactions such as in $Cd(H_2O)_2Ni(CN)_4 \cdot (H_2O)_4$[22]. Rather, the hydrogen-bonding framework of the water molecules appears to form kinked strands of O_8 rings, which run colinear to the *b* axis. However, when the split position of the O5 atoms and of the hydrogen atoms on O2 is taken into account the strands are interrupted, and the water structure is better described as being comprised of individual rings or chain segments. Then the structure of the water layer (ordered by rapid cooling of the crystal) resembles more that of a frozen liquid with a temperature-dependent formation of larger H_2O clusters[20].

Figure 10. View from above of a water layer in **8** · 6 H_2O at 293 (**a**) and 160 K (**b**). The three crystallographically different oxygen positions are represented differently in **a** (O atoms related by disorder are shown alike as void and crossed circles). In the area of the unit cell in **a** all oxygen centers are shown, outside two out of the three respective disordered positions were removed for a visualization of the possible H_2O clustering [—— d(O—O) = 2.54–2.66, – – – d(O—O) = 2.95–3.02 Å, unconnected oxygen centers are more than 3.1 Å apart]. To allow a better comparison of the order/disorder the same representation and unit cell content were also adopted in **b**, despite the fact that the different space group at 160 K gives rise to five crystallographically indepented oxygen positions (see Figure 11)

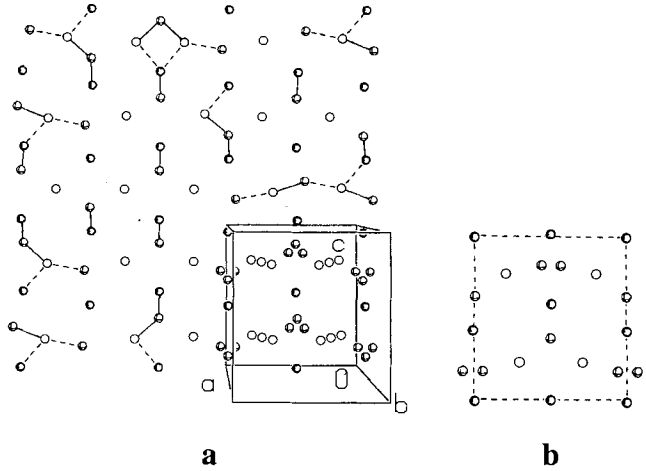

Scanning Electron Microscopy

The surface structure of **8** after the loss of water of crystallization from a cubic crystal plate has been studied by scanning electron microscopy (SEM). The SEM pictures

Figure 11. View from above of a water layer in **8** · 6 H_2O at 160 K with the hydrogen-bonding network (dashed lines) and including the hydrogen-bonded nitrogen atoms of the triazolyl rings (shaded circles, PLUTON[14]). The atomic numbering scheme is illustrated. O3, O1, and O2 lie on a mirror plane (symmetry operation x, 0.5 − y, z); for the symmetry labels, see Table 4

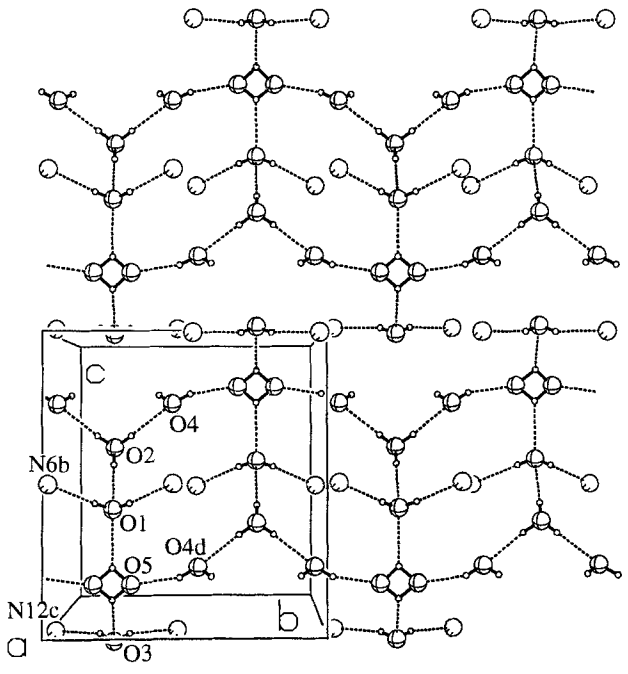

are displayed and correlated with the crystal morphology and packing in Figure 12. The rectangular sides of the cubic plate show fine tears with the same directionality running parallel to the long edges (Figure 12 **a**). The square-basal plane of the plate, however, has the appearance of a cracked brick wall, "built" in line with the diagonal of the plane (Figure 12 **b**). Precession-camera photographs allowed us to establish a correlation between the crystallographic axes and the crystal morphology: The longest axis b stands perpendicularly on the square-basal plane or parallel to the short edges, while the approximately equal a and c axis (cf. Table 6, room-temperature structure) are positioned along the plane diagonals or through the short edges of the crystal plate (see Figure 12). Picturing the unit cell relative to its position within the cubic plate provides then an understanding of the surface fractures: The water layers run parallel to the ac plane (**a**) or parallel to the long rectangular edges, and the metal-complexes are "lined-up" along a and c in their layers (**b**). Diffusion of the water out of the crystal lattice then leaves molecular-sized openings which can, of course, not be detected with the available magnification, but an imperfect collapse or closing of the gaps between the metal complex layers along b leads to the larger, visible cracks in Figure 12 **a**, and gives rise to the brick pattern in **b**. The latter emerges since the intermolecular interaction between the complexes is not the same along a and c (at this point it was not possible to decide which axis, a or c, corresponded to which diagonal) and since the closure of the gap between the layers occurs stepwise with the water diffusion progressing from the crystal surfaces to the interior.

Table 4. Hydrogen-bonding scheme in the low-temperature structure of **8** · 6 H_2O[a]

Donor–H···Acceptor	D···A [Å]	D–H [Å]	H···A [Å]	D–H···A [°]
O1—H11···N6b	2.864(5)	0.79(4)	2.08(4)	177(5)
O2—H21···O1	2.874(8)	0.82(6)	2.06(6)	179(8)
O2—H22···O4	2.752(7)	0.86(7)	1.97(9)	149(10)
O3—H31···N12c	2.860(5)	0.78(4)	2.11(5)	161(6)
O4d—H41d···O5	2.58(1)	0.85(6)	1.85(6)	143(7)
O5—H52···O1	2.897(9)	0.96(5)	2.20(8)	129(5)
O5—H51···O3	2.878(9)	1.02(5)	2.06(8)	135(3)

[a] Symmetry transformations used to generate equivalent atoms: b = $-x$ + 0.5, $-y$, z − 0.5; c = $-x$, $-y$, $-z$ + 1; d − x, $-y$, + 1, $-z$ + 1. − All other O···O and O···N contacts are above 3.23 Å.

Conclusions

The novel bis(1,2,4-triazolyl)borate ligand **2** exhibits the expected bridging coordination mode for poly(triazolyl)-borates by the exodentate nitrogen atoms and, thereby, illustrates the chelate effect at work in the molecular complexes formed with the tris(1,2,4-triazolyl)borate ligand **1**. The crystal phases of the metal-bis(triazolyl)borate systems are stabilized by water molecules which in turn are organized into an ordered hydrogen-bonded network of isolated or edge-sharing six-membered rings by the template effect of the endodentate nitrogen atoms and the metal-aqua ligands.

The X-ray structure of the solvated octahedral chelate complex $[Ni\{HB(C_2H_2N_3)_3\}_2] \cdot 6\ H_2O$ shows complex-containing layers sandwiching weakly hydrogen-bonded water layers. The room-temperature structure, despite the highly disordered water molecules, supports a cluster-model description for two-dimensional liquid water. At 160 K, these water molecules organize into a fully ordered hydrogen-bonded network. All of the hydrogen atoms could be refined and thus the cluster-like nature of the 2-D water layer revealed in intricate detail.

This work was supported by the *Deutsche Forschungsgemeinschaft* (grant Ja466/4-1), the *Fonds der Chemischen Industrie*, and the *Freunde der TU Berlin*. We express our appreciation and thanks to Prof. *H. Schumann* for his generous and encouraging support and to Mrs. *M. Borowski* for collecting the crystallographic data set of **7**. The help of Dr. *W. Günther* and (in part) Dr. *H. W. Sichting* in obtaining the magnetochemical data and the precession-camera photographs is appreciated. We thank Mr. *G. Urmann* from the *Heinrich-Hertz-Institut für Nachrichtentechnik Berlin GmbH* for the SEM photographs.

Experimental

Bidistilled or de-ionized water was used as a solvent. − CHN: Perkin-Elmer Series II CHNS/O Analyzer 2400. − IR: Perkin-Elmer 580B or Nicolet Magna 750. − MS: Varian MAT 311A. − NMR: Bruker ARX 200. − Susceptibility measurements: Faraday magnetic balance and AC susceptometer Lakeshore Model 7000. − Precession camera: STOE, Mo-K_α radiation. − SEM: CamScan;

Figure 12. Crystal morphology with relative positions of crystal axes and unit cell (room temperature) and SEM surface structures of a dried cubic crystal plate of **8**, (**a**) viewed from above the rectangular side (parallel to the *ac* plane) and (**b**) viewed from above the square basal plane (along *b*). In the unit cell **a** only the oxygen centers (crossed circles) are shown for the water molecules and only the "middle" oxygen center which occupies a special position is displayed for the disordered H_2O molecules (cf. Figure 10). In the view from above a metal-complex layer in **b** the water molecules have been omitted for clarity

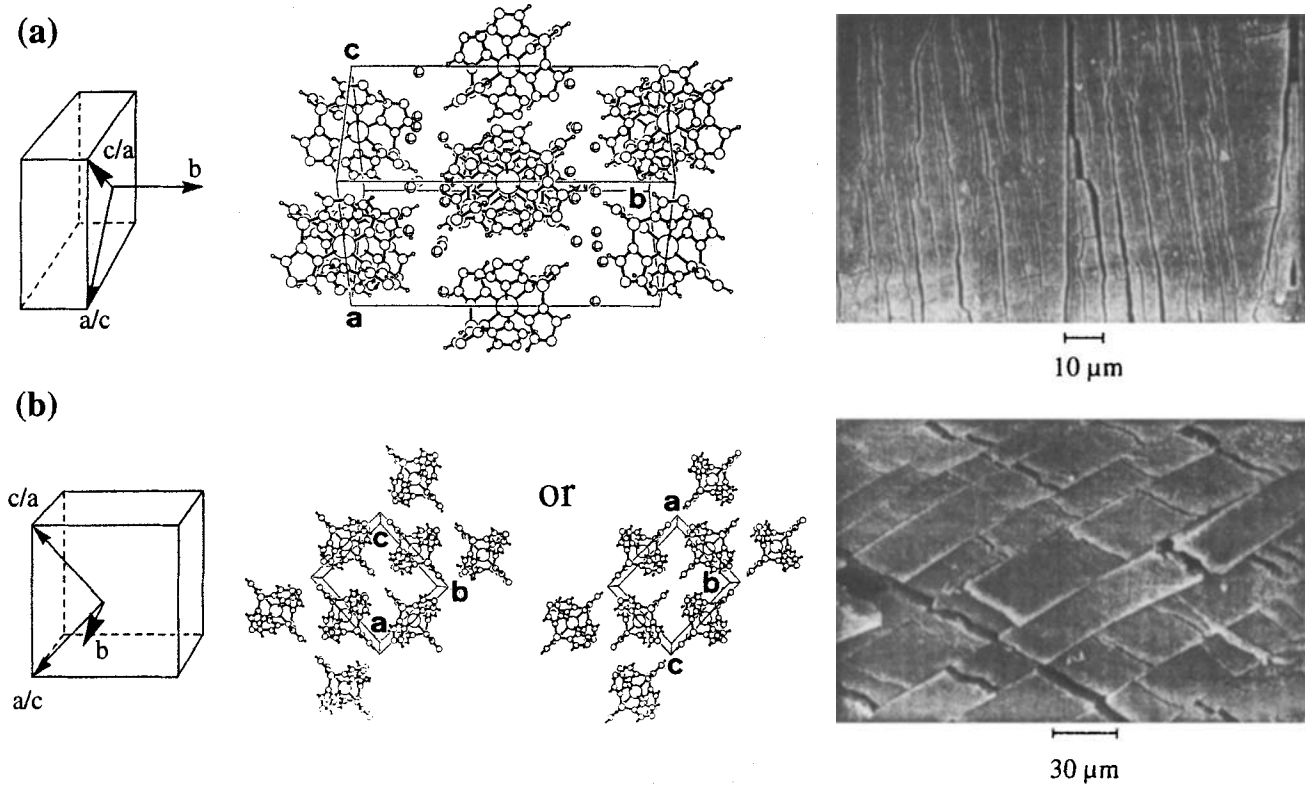

the dried crystal plate was mounted on the rectangular side and sprayed with a 10–15 nm gold layer. – The potassium salt of **1** was synthesized from KBH_4 and triazole according to refs.[4,12].

K[H₂B(C₂H₂N₃)₂] (**4**): In a 100-ml flask equipped with a gas meter an intimate mixture of 2.1 g (40 mmol) of KBH_4 and 5.9 g (85 mmol) of triazole was heated to about 120°C. At this temp. a brisk hydrogen evolution started and in a few minutes about 95% (≈1.9 l) of the estimated hydrogen was evolved, after which the gas evolution quickly subsided. A porous soft material was obtained. The reaction was allowed to continue for some time during which, however, only an additional 0.02 l of hydrogen was collected. After cooling to room temp. the solid was washed three times with 25 ml of warm tetrahydrofuran to remove unreacted triazole. Drying in vacuo yielded 6.7 g (90%) of a snow-white powder which was used as such for the synthesis of the transition-metal complexes. Analytical samples were recrystallized from methanol or ethanol; m.p. 293–295°C (dec.). – IR (KBr): $\tilde{\nu}$ = 3218 cm^{-1} m, 3205 m, 2435 m, 2405 m, 2350 m, 2290 w, 2267 w, 1503 s, 1411 w, 1312 m, 1265 s, 1208 m, 1178 s, 1155 vs, 1128 w, 1121 w, 1028 m, 1021 m, 962 w, 884 s, 873 w, 725 w, 685 s, 674 s, 676 w, 658 w, 641 m. – ^1H NMR (D_2O): δ = 7.92 (s, 1 H, "C1"-H), 8.26 (s, 1 H, "C2"-H) (BH signal could not be observed due to its broad resonance because of quadrupolar coupling and relaxation effects from the boron atom[23]). – ^{13}C NMR (D_2O): δ = 149.2 ("C2"), 152.4 ("C1"). (A direct assignment of the two ^1H- or ^{13}C-NMR signals to the two different hydrogen or carbon atoms was not possible. From a comparison with the thoroughly studied poly(*pyrazolyl*)borate spectra[24] we infer the assignments given above. For the "C1"/"C2"-type description cf. the atom numbering in Figures 2 or 3.) – $C_4H_6BKN_6$ (188.0): calcd. C 25.55, H 3.22, K 20.79, N 44.69; found C 25.77, H 3.56, K 20.01, N 43.80.

{[Mn(H₂O)₂{μ-H₂B(C₂H₂N₃)₂}₂] · 4 H₂O}∞ (**5**): A solution of 0.06 g (0.5 mmol) of anhydrous $MnCl_2$ in 10 ml of water was carefully overlayered in a test tube with a solution of 0.19 g (1.0 mmol) of **4** in 20 ml of water. Slow diffusion of the solutions of the starting compounds then led to the formation of **5** as colorless crystals. Yield 0.05 g (22%), m.p. > 260°C. – IR (KBr): $\tilde{\nu}$ = 3403 cm^{-1} s (br, OH), 3145 vw, 2926 vw, 2854 vw, 2444 m, 2410 m, 2349 w, 2269 w, 1738 vw, 1666 w, 1637 w, 1525 sh, 1514 s, 1432 w, 1342 w to m, 1283 m, 1272 m, 1180 m, 1148 vs, 1124 s, 1023 m, 997 m, 990 m, 976 sh, 890 m, 871 w, 723 vw, 674 m, 663 w, 627 m. – Magnetic moment: μ = 5.7 μ_B (300 K). – $C_8H_{24}B_2MnN_{12}O_6$ (460.9): calcd. C 20.85, H 5.25, N 36.47; found C 20.30, H 5.04, N 36.49 (hydrated, crystalline material).

{[M(H₂O)₂{μ-H₂B(C₂H₂N₃)₂}₂] · n H₂O}∞ [M = Ni, *n* undetermined (**6**); Cu, *n* = 6 (**7**)]: A solution of 1.0 mmol of the transition-metal salt (0.13 g of $NiCl_2$ or 0.25 g of $CuSO_4 \cdot 5\ H_2O$) in 10 ml of water was carefully overlayered in a test tube with a solution of 0.38 g (2.0 mmol) of the potassium salt of **2** in 20 ml of water. No crystalline material, only a blue-violet (**6**) or dark blue (**7**) voluminous amorphous precipitate formed which after filtration was completely dissolved in 3 ml of concentrated aqueous ammonia (25%) to afford a clear violet or deep blue solution, respectively. Slow solvent evaporation gave lilac needles (**6**) or dark blue crystal plates (**7**). When removed from the water phase the crystals quickly turned opaque with loss of crystallinity due to the evaporation of water of crystallization.

Compound **6** (dried material): Yield 0.20 g (50%), m.p. >260°C. – IR (KBr): $\tilde{\nu}$ = 3360 cm^{-1} m (br, OH), 3185 vw, 2924 vw, 2455 m, 2434 m, 2370 w, 2277 w, 1766 w, 1656 sh, 1622 m, 1505 s, 1436 w, 1420 w, 1317 m, 1284 s, 1235 w, 1189 m, 1155 s, 1137 m, 1042 s, 986 w, 970 w, 962 m, 888 m, 870 m, 723 w, 673 s, 634 vw, 598 w. – $C_8H_{16}B_2N_{12}NiO_2$ (392.6): calcd. C 24.45, H 4.11, N 42.82; found C 23.59, H 4.98, N 43.77.

Compound **7** (dried material): Yield 0.10 g (25%), m.p. 202–205°C. – IR (KBr): $\tilde{\nu}$ = 3383 cm^{-1} m (br, OH), 3132 m, 2425 m (BH), 2288 w, 1660 w (br), 1520 s, 1443 w, 1333 w, 1285 m, 1185 sh, 1153 s, 1121 s, 1024 m, 1014 m, 1004 m, 876 m, 726 w, 671 s, 650 w. – Magnetic moment: μ = 2.0 μ_B (300 K). – $C_8H_{16}B_2CuN_{12}O_2$ (399.3): calcd. C 24.06, H 4.04, N 42.09; found C 25.75, H 3.45, N 44.05.

[Ni{HB(C$_2$H$_2$N$_3$)$_2$}$_2$] (**8**): A solution of 0.23 g (1.0 mmol) of $NiCl_2 \cdot 6\ H_2O$ in 10 ml of water was carefully overlayered in a test tube with a solution of 0.50 g (2.0 mmol) of K[HB($C_2H_2N_3$)$_3$] (potassium salt of **1**) in 20 ml of water. Some amorphous material precipitated in this process. Upon slow diffusion of the solutions of the starting compounds the originally light-green nickel chloride solution turned blue, the upper colorless borate layer became light pink-violet, and the first red-violet crystals of **8** · 6 H_2O started to form within 24 h. The reaction and process of crystallization were concluded within 2 weeks to give analytically pure, well-shaped crystals. Except for the X-ray diffraction studies, the solvent-free lilac-colored complex obtained upon air-drying of the crystalline material was analyzed. Yield 0.30 g (61%), m.p. >260°C (not determined). – IR (CsI): $\tilde{\nu}$ = 3129 cm^{-1} w, 3100 m, 3089 m (C–H), 3000 vw, 2518 w, 2495 m (B–H), 1507 s, 1415 m, 1328 m, 1322 m, 1291 s, 1229 w, 1218 w, 1202 m, 1193 m, 1150 s, 1102 w, 1049 m, 1029 s, 969 sh, 964 s, 925 w, 905 sh, 894 m, 872 m, 787 w, 730 sh, 719 s, 674 s, 665 sh. – MS (EI, 70 eV, 240°C), *m/z* (%): 490 (100, $M^{+\bullet}$), 422 (35, $[M - C_2H_2N_3]^+$), 420 (14, $[M - C_2H_2N_3 - 2H]^+$), 353 (92, $[M - 2\ C_2H_2N_3 - H]^+$), 352 (62, $[M - 2\ C_2H_2N_3 - 2H]^{+\bullet}$), 326 (5, $[M - 2\ C_2H_2N_3 - H - HCN]^+$), 274 (75, $[M - HB(C_2H_2N_3)_3]^+$ = $[Ni\{HB(C_2H_2N_3)_3\}]^+$), 219 (24, $[Ni\{HB(C_2H_2N_3)_3\} - 2\ HCN - H]^{+\bullet}$), 206 (7, $[Ni\{HB(C_2H_2N_3)_3\} - C_2H_2N_3]^{+\bullet}$), 205 (7, $[Ni\{HB(C_2H_2N_3)_3\} - C_2H_2N_3 - H]^+$), 178 (17, $[Ni\{HB(C_2H_2N_3)_3\} - C_2H_2N_3 - H - HCN]^+$), 177 (20, $[Ni\{HB(C_2H_2N_3)_3\} - C_2H_2N_3 - 2H - HCN]^{+\bullet}$), 165 (15), 152 (12, $[Ni\{HB(C_2H_2N_3)_3\} - C_2H_2N_3 - 2\ HCN]^{+\bullet}$), 129 (15), 69 (10, $[C_2H_3N_3]^{+\bullet}$) (peaks listed refer to the most abundant isotope combination ^{58}Ni, ^{11}B). – Magnetic moment: μ = 3.0 μ_B (300 K). – $C_{12}H_{14}B_2N_{18}Ni$ (490.7): calcd. C 29.37, H 2.88, N 51.38; found C 29.18, H 2.57, N 51.92.

X-Ray Structure Determinations: STOE four-circle diffractometer for **5** [ω scan (5° ≤ 2Θ ≤ 50°, −9 ≤ *h* ≤ 9, 0 ≤ *k* ≤ 18, 0 ≤ *l* ≤ 10] and **8** · 6 H_2O [ambient temp., 293 K, ω scan (4° ≤ 2Θ ≤ 54°, −16 ≤ *h* ≤ 16, 0 ≤ *k* ≤ 30, 0 ≤ *l* ≤ 16)]; CAD4, Enraf-Nonius four-circle diffractometer for **7** [ω-2Θ scan (5° ≤ 2Θ ≤ 55°, 0 ≤ *h* ≤ 11, 0 ≤ *k* ≤ 16, 0 ≤ *l* ≤ 21)] and **8** · 6 H_2O [low temperature, 160 K; ω-2Θ scan (2° ≤ 2Θ ≤ 50°, 0 ≤ *h* ≤ 12, 0 ≤ *k* ≤ 24, 0 ≤ *l* ≤ 13)]; the crystals of **5**, **7**, and **8** · 6 H_2O were measured in capillaries at room temp. (293 K), for the low-temperature data collection of **8** · 6 H_2O the crystal was taken out of the aqueous phase and quickly transferred to the cold nitrogen stream of the diffractometer. Mo-K_α radiation (λ = 71.069 pm, graphite monochromator). Structure solutions were performed by direct methods (SHELXS-86[25]). Refinement: Full-matrix least-squares (SHELXL-93[25]) with all non-hydrogen atoms anisotropic. The hydrogen atoms were located and refined, except for those in the disordered water molecules of the room-temperature structure of **8** · 6 H_2O. Crystal data are listed in Table 5 for **5** and **7** and in Table 6 for the two temperature forms of **8** · 6 H_2O[26].

Table 5. Crystal data for compounds **5** and **7**

	5	**7**
Formula	$C_4H_{12}BMn_{0.5}N_6O_3$ ($C_8H_{24}B_2MnN_{12}O_6$)	$C_8H_{28}B_2CuN_{12}O_8$
Mol. mass [g mol^{-1}]	230.48 (460.96)	505.59
Crystal size [mm]	1.0 · 0.6 · 0.1	0.5 · 0.2 · 0.1
Crystal system	Monoclinic	Orthorhombic
Space group	$P2_1/n$ (No. 14)	*Pccn* (No. 56)
a [Å]	8.140(3)	9.483(2)
b [Å]	15.953(6)	14.080(2)
c [Å]	8.918(4)	17.688(3)
β [°]	105.95(3)	90.00(2)
V [$Å^3$]	1113.4(8)	2361.9(7)
Z	4	4
$D_{calcd.}$ [g cm^{-3}]	1.375	1.422
F(000)	478	1052
μ(MoKα) [mm^{-1}]	0.641	0.962
Absorption correction: max.; min.; av.	DIFABS 1.294; 0.716; 0.970	DIFABS 1.002; 0.498; 0.673
Measured reflections	2206	1839
Unique reflections	1823 (R_{int} = 0.0268)	1104 (R_{int} = 0.1416)
Data for refinement (n)	1818	1104
Parameters refined (p)	181	193
Δρ [a]: max;min [e $Å^{-3}$]	0.25; -0.26	0.51; -0.56
R1; *wR2* [b] [$I > 2\sigma(I)$]	0.0413; 0.0746	0.0846; 0.1273
Goodness of fit [c]	0.968	1.208
Weighting scheme, *w*; *a*; *b* [d]	0.000; 0.000	0.0221; 3.48

[a] Largest difference peak and hole. – [b] $R1 = (\Sigma \| F_o \| - \| F_c \|)/\Sigma |F_o|$; $wR2 = [\Sigma[w(F_o^2 - F_c^2)^2]/\Sigma [w(F_o^2)^2]]^{1/2}$. – [c] Goof = $[\Sigma [w(F_o^2 - F_c^2)^2]/(n - p)]^{1/2}$. – [d] $w = 1/[\sigma^2(F_o^2) + (a \cdot P)^2 + b \cdot P]$ where $P = [\max(F_o^2 \text{ or } 0) + 2 \cdot F_c^2]/3$.

Table 6. Crystal data for compound **8** · 6 H_2O at 293 and 160 K

Temperature	293 K	160 K
Formula	$C_{12}H_{26}B_2N_{18}O_6Ni$	
Mol. mass [g mol^{-1}]	598.82	
Crystal size [mm]	0.5 · 0.5 · 0.5	0.2 · 0.2 · 0.1
Crystal system	Orthorhombic	
Space group	*Cmca* (No. 64)	*Pmnb* (*Pnma*; No. 62)
a [Å]	10.890(7)	20.769(5)
b [Å]	20.998(13)	10.801(2)
c [Å]	11.754(8)	11.635(3)
V [$Å^3$]	2688(3)	2610(1)
Z	4	4
$D_{calcd.}$ [g cm^{-3}]	1.480	1.524
F(000)	1240	
μ(MoKα) [mm^{-1}]	0.768	0.791
Absorption correction: max.; min.; av.	none –	DIFABS 1.234; 0.879; 0.980
Measured reflections	1610	2230
Unique reflections	1540 (R_{int} = 0.0176)	2227 (R_{int} = 0.0000)
Data for refinement (n)	1534	2185
Parameters refined (p)	138	262
Δρ [a]: max;min [e $Å^{-3}$]	0.33; -0.76	0.38; -0.33
R1; *wR2* [b] [$I > 2\sigma(I)$]	0.0389; 0.0956	0.0553; 0.0902
Goodness of fit [c]	1.044	1.084
Weighting scheme, *w*; *a*; *b* [d]	0.059; 0.85	0.010; 9.90

[a–d] See Table 5.

☆ Dedicated to Prof. Dr. *Hubert Schmidbaur* on the occasion of his 60th birthday.

[1] C. Janiak, *J. Chem. Soc., Chem. Commun.* **1994**, 545–547.

[2] C. Janiak, *Chem. Ber.* **1994**, *127*, 1379–1385.

[3] C. Janiak, H. Hemling, *J. Chem. Soc., Dalton Trans.* **1994**, 2947–2952.

[4] G. G. Lobbia, F. Bonati, P. Cecchi, *Synth. React. Inorg. Met.-Org. Chem.* **1991**, *21*, 1141–1151.

[5] C. Janiak, L. Esser, *Z. Naturforsch., Teil B*, **1993**, *48*, 394–396.

[6] C. Janiak, T. G. Scharmann, P. Reich, K.-W. Brzezinka, *Chem. Ber.*, in press.

[7] Reviews: S. Trofimenko, *Chem. Rev.* **1993**, *93*, 943–980; P. K. Byers, A. J. Canty, R. T. Honeyman, *Adv. Organomet. Chem.* **1992**, *34*, 1–65; K. Niedenzu, S. Trofimenko, *Top. Curr. Chem.* **1986**, *131*, 1–37; S. Trofimenko, *Progr. Inorg. Chem.* **1986**, *34*, 115–210.

[8] K.-B. Shiu, J. Y. Lee, Y. Wang, M.-C. Cheng, S.-L. Wang, F.-L. Liao, *J. Organomet. Chem.* **1993**, *453*, 211–219.

[9] K. Liu, J. G. Loeser, M. J. Elrod, B. C. Host, J. A. Rzepiela, N. Pugliano, R. J. Saykally, *J. Am. Chem. Soc.* **1994**, *116*, 3507–3512; I. I. Vaisman, F. K. Brown, A. Tropsha, *J. Phys. Chem.* **1994**, *98*, 5559–5564; M. Vedamuthu, S. Singh, G. W. Robinson, *ibid.* **1994**, *98*, 2222–2230; I. M. Svishchev, P. G. Kusalik, *ibid.* **1994**, *98*, 728–733; D. J. Wales, *J. Am. Chem. Soc.* **1993**, *115*, 11180–11190.

[10] *Water and Biological Macromolecules* (Ed.: E. Westhoff), MacMillan, London, **1993**; G. A. Jeffrey, W. Saenger, *Hydrogen Bonding in Biological Structures*, Springer-Verlag, New York, **1991**, and references therein; R. L. Harlow, *J. Am. Chem. Soc.* **1993**, *115*, 9838–9839.

[11] M. D. Marcos, P. Amorós, D. Beltrán, A. Beltrán, *Inorg. Chem.* **1994**, *33*, 1220–1226; A. H. Cowley, F. P. Gabbai, D. A. Atwood, C. J. Carrano, L. M. Mokry, M. R. Bond, *J. Am. Chem. Soc.* **1994**, *116*, 1559–1560; N. Uchida, S. Kittaka, *J. Phys. Chem.* **1994**, *98*, 2129–2133; S. Nishikiori, T. Iwamoto, *J. Chem. Soc., Chem. Commun.* **1993**, 1555–1556.

[12] S. Trofimenko, *J. Am. Chem. Soc.* **1967**, *89*, 3170–3177; *Inorg. Synth.* **1970**, *12*, 99–106.

[13] A. Weiss, H. Witte, *Magnetochemie*, Verlag Chemie, Weinheim, **1973**; F. E. Mabbs, D. J. Machin, *Magnetism and Transition Metal Complexes*, Chapman and Hall, London, **1973**.

[14] A. L. Spek, *PLATON-93* and *PLUTON-92 graphics program*, University of Utrecht, The Netherlands, **1993** and **1992**, respectively; A. L. Spek, *Acta Crystallogr., Sect. A*, **1990**, *46*, C34.

[15] M. Ferigo, P. Bonhôte, W. Marty, H. Stoeckli-Evans, *J. Chem. Soc., Dalton Trans.* **1994**, 1549–1554.

[16] D. D. MacNicol, J. J. McKendrick, D. R. Wilson, *Chem. Soc. Rev.* **1978**, *7*, 65–87, and references therein.

[17] I. Goldberg, *Top. Curr. Chem.* **1988**, *149*, 1–44; F. H. Herbstein, *ibid.* **1987**, *140*, 107–141.

[18] W. Saenger, K. Lindner, *Angew. Chem.* **1980**, *92*, 404–405; *Angew. Chem. Int. Ed. Engl.* **1980**, *19*, 398–399.

[19] L. Pauling, *The Nature of the Chemical Bond*, 3rd ed., Cornell University Press, Ithaca, **1960**, p. 260; *Handbook of Chemistry and Physics*, 62nd ed., CRC Press, Cleveland, **1981–1982**, p. D-166.

[20] H. A. Scheraga, *Acc. Chem. Res.* **1979**, *12*, 7–14, and references therein. See also: G. Geiseler, *Z. Chem.* **1978**, *18*, 1–8; K. Tempelhoff, *ibid.* **1977**, *17*, 121–131; E. Wicke, *Angew. Chem.* **1966**, *78*, 1–19; *Angew. Chem. Int. Ed. Engl.* **1966**, *5*, 106–124.

[21] W. F. Kuhs, J. L. Finney, C. Vettier, D. V. Bliss, *J. Chem. Phys.* **1984**, *81*, 3612–3623, and references therein.

[22] K.-M. Park, R. Kuroda, T. Iwamoto, *Angew. Chem.* **1993**, *105*, 939–941; *Angew. Chem. Int. Ed. Engl.* **1993**, *32*, 884–886, and references therein.

[23] D. L. Reger, S. S. Mason, A. L. Rheingold, R. L. Ostrander, *Inorg. Chem.* **1993**, *32*, 5216–5222; R. K. Harris, *Nuclear Magnetic Resonance Spectroscopy*, Pitman, London, **1983**, chapter 5-14, p. 138–141.

[24] C. Lopez, R. M. Claramunt, D. Sanz, C. F. Foces, F. H. Cano, R. Faure, E. Cayon, J. Elguero, *Inorg. Chim. Acta* **1990**, *176*, 195–204.

[25] G. M. Sheldrick, *SHELXL-93, Program for Crystal Structure Refinement*, Göttingen, **1993**; *SHELXS-86, Program for Crystal Structure Solution*, Göttingen, **1986**.

[26] Further details of the crystal structure determinations are available on request from the Fachinformationszentrum Karlsruhe, Gesellschaft für wissenschaftlich-technische Information mbH, D-76344 Eggenstein-Leopoldshafen, on quoting the depository number CSD-58672, the authors, and the journal citation.

[371/94]